

Measurement of Exclusive Baryon-Antibaryon Decays of χ_{cJ} Mesons

P. Naik,¹ J. Rademacker,¹ D. M. Asner,² K. W. Edwards,² J. Reed,² R. A. Briere,³
 T. Ferguson,³ G. Tatishvili,³ H. Vogel,³ M. E. Watkins,³ J. L. Rosner,⁴ J. P. Alexander,⁵
 D. G. Cassel,⁵ J. E. Duboscq,⁵ R. Ehrlich,⁵ L. Fields,⁵ L. Gibbons,⁵ R. Gray,⁵
 S. W. Gray,⁵ D. L. Hartill,⁵ B. K. Heltsley,⁵ D. Hertz,⁵ J. M. Hunt,⁵ J. Kandaswamy,⁵
 D. L. Kreinick,⁵ V. E. Kuznetsov,⁵ J. Ledoux,⁵ H. Mahlke-Krüger,⁵ D. Mohapatra,⁵
 P. U. E. Onyisi,⁵ J. R. Patterson,⁵ D. Peterson,⁵ D. Riley,⁵ A. Ryd,⁵ A. J. Sadoff,⁵
 X. Shi,⁵ S. Stroiney,⁵ W. M. Sun,⁵ T. Wilksen,⁵ S. B. Athar,⁶ R. Patel,⁶ J. Yelton,⁶
 P. Rubin,⁷ B. I. Eisenstein,⁸ I. Karliner,⁸ S. Mehrabyan,⁸ N. Lowrey,⁸ M. Selen,⁸
 E. J. White,⁸ J. Wiss,⁸ R. E. Mitchell,⁹ M. R. Shepherd,⁹ D. Besson,¹⁰ T. K. Pedlar,¹¹
 D. Cronin-Hennessy,¹² K. Y. Gao,¹² J. Hietala,¹² Y. Kubota,¹² T. Klein,¹² B. W. Lang,¹²
 R. Poling,¹² A. W. Scott,¹² P. Zweber,¹² S. Dobbs,¹³ Z. Metreveli,¹³ K. K. Seth,¹³
 A. Tomaradze,¹³ J. Libby,¹⁴ A. Powell,¹⁴ G. Wilkinson,¹⁴ K. M. Ecklund,¹⁵ W. Love,¹⁶
 V. Savinov,¹⁶ H. Mendez,¹⁷ J. Y. Ge,¹⁸ D. H. Miller,¹⁸ I. P. J. Shipsey,¹⁸ B. Xin,¹⁸
 G. S. Adams,¹⁹ M. Anderson,¹⁹ J. P. Cummings,¹⁹ I. Danko,¹⁹ D. Hu,¹⁹ B. Moziak,¹⁹
 J. Napolitano,¹⁹ Q. He,²⁰ J. Insler,²⁰ H. Muramatsu,²⁰ C. S. Park,²⁰ E. H. Thorndike,²⁰
 F. Yang,²⁰ M. Artuso,²¹ S. Blusk,²¹ S. Khalil,²¹ J. Li,²¹ R. Mountain,²¹ S. Nisar,²¹
 K. Randrianarivony,²¹ N. Sultana,²¹ T. Skwarnicki,²¹ S. Stone,²¹ J. C. Wang,²¹
 L. M. Zhang,²¹ G. Bonvicini,²² D. Cinabro,²² M. Dubrovin,²² and A. Lincoln²²

(CLEO Collaboration)

¹University of Bristol, Bristol BS8 1TL, UK

²Carleton University, Ottawa, Ontario, Canada K1S 5B6

³Carnegie Mellon University, Pittsburgh, Pennsylvania 15213, USA

⁴Enrico Fermi Institute, University of Chicago, Chicago, Illinois 60637, USA

⁵Cornell University, Ithaca, New York 14853, USA

⁶University of Florida, Gainesville, Florida 32611, USA

⁷George Mason University, Fairfax, Virginia 22030, USA

⁸University of Illinois, Urbana-Champaign, Illinois 61801, USA

⁹Indiana University, Bloomington, Indiana 47405, USA

¹⁰University of Kansas, Lawrence, Kansas 66045, USA

¹¹Luther College, Decorah, Iowa 52101, USA

¹²University of Minnesota, Minneapolis, Minnesota 55455, USA

¹³Northwestern University, Evanston, Illinois 60208, USA

¹⁴University of Oxford, Oxford OX1 3RH, UK

¹⁵State University of New York at Buffalo, Buffalo, New York 14260, USA

¹⁶University of Pittsburgh, Pittsburgh, Pennsylvania 15260, USA

¹⁷University of Puerto Rico, Mayaguez, Puerto Rico 00681

¹⁸Purdue University, West Lafayette, Indiana 47907, USA

¹⁹Rensselaer Polytechnic Institute, Troy, New York 12180, USA

²⁰University of Rochester, Rochester, New York 14627, USA

²¹Syracuse University, Syracuse, New York 13244, USA

²²Wayne State University, Detroit, Michigan 48202, USA

(Dated: June 10, 2008)

Abstract

Using a sample of 2.59×10^7 $\psi(2S)$ decays collected by the CLEO-c detector, we present results of a study of χ_{cJ} ($J=0,1,2$) decays into baryon-antibaryon final states. We present the world's most precise measurements of the $\chi_{cJ} \rightarrow p\bar{p}$ and $\chi_{cJ} \rightarrow \Lambda\bar{\Lambda}$ branching fractions, and the first measurements of χ_{c0} decays to other hyperons. These results illuminate the decay mechanism of the χ_c states.

PACS numbers: 13.25.Gv, 14.40.Gx

In the standard quark model, the χ_{cJ} ($J = 0, 1, 2$), mesons are $c\bar{c}$ states in an $L = 1$ configuration. The χ_{cJ} mesons are not produced directly in e^+e^- annihilations. However, the large branching fractions of $\psi(2S) \rightarrow \chi_{cJ}\gamma$ make e^+e^- collisions at the $\psi(2S)$ energy a very clean environment for χ_{cJ} investigation.

The available data on the decays of the χ_{cJ} mesons into baryon-antibaryon pairs has so far been very limited. The easiest of these final states to detect and measure is $p\bar{p}$ [1]. The partial width for $\chi_{c0} \rightarrow p\bar{p}$ was originally predicted to be zero in some models due to the Helicity Selection Rule [2]. However, this rule has long been known to be strongly violated. More recent work has concentrated on the importance of the Color Octet Mechanism (COM), which treats the χ_c states as more than just pure $q\bar{q}$ states and incorporates octet operators in the transition matrix elements to a given final state in order to calculate two-body exclusive decay rates [3]. In particular, Wong [4] used the COM to explain the high rate of $\chi_{cJ} \rightarrow p\bar{p}$ and made predictions for $\chi_{cJ} \rightarrow \Lambda\bar{\Lambda}$. However, these predictions fell well below the low-statistics measurements from BES [5] that imply $\mathcal{B}(\chi_c \rightarrow \Lambda\bar{\Lambda})/\mathcal{B}(\chi_c \rightarrow p\bar{p}) \approx 2$ to 4 for all three χ_c states. It has since been postulated that such large ratios can be explained without using the COM, and, instead including a more detailed quark model of the daughter products [6]. However, the resulting predictions depend greatly on the details of this model, and it is clear that more experimental input is needed. In this paper, we analyze a large sample of $\psi(2S)$ decays and present results on two-body decays of the χ_{cJ} mesons into $p\bar{p}$, $\Lambda\bar{\Lambda}$, $\Sigma^0\bar{\Sigma}^0$, $\Sigma^+\bar{\Sigma}^+$, $\Xi^-\bar{\Xi}^-$, and $\Xi^0\bar{\Xi}^0$.

The data were taken by the CLEO-c detector [7] operating at the Cornell Electron Storage Ring with e^+e^- collisions at a center of mass energy corresponding to the $\psi(2S)$ mass of 3.686 GeV/ c^2 . The data correspond to an integrated luminosity of 56.3 pb $^{-1}$, and the total number of $\psi(2S)$ events is calculated as 2.59×10^7 , determined according to the method described in [8].

Photons were detected using the CsI crystal calorimeter [9], which has an energy resolution of 2.2% at 1 GeV, and 5% at 100 MeV. To discriminate protons from kaons and pions, we combined specific ionizations (dE/dx) measured in the drift chamber and log-likelihoods obtained from the ring-imaging Čerenkov detector (RICH) [10] to form a log-likelihood difference: $\mathcal{L}(p - \pi) = \mathcal{L}_{RICH}(p) - \mathcal{L}_{RICH}(\pi) + \sigma_{dE/dx}^2(p) - \sigma_{dE/dx}^2(\pi)$, where negative $\mathcal{L}(p - \pi)$ implies the particle is more likely to be proton than a pion. For all protons in the events we require $\mathcal{L}(p - \pi) < 0$ and $\mathcal{L}(p - K) < 0$. This is a very efficient requirement.

We reconstruct the hyperons in the following decay modes: $\Lambda \rightarrow p\pi^-$ (branching fraction 63.9%) [1], $\Sigma^+ \rightarrow p\pi^0$ (51.6%), $\Sigma^0 \rightarrow \Lambda\gamma$ (100%), $\Xi^- \rightarrow \Lambda\pi^-$ (99.9%), and $\Xi^0 \rightarrow \Lambda\pi^0$ (99.5%). Our hyperon detection follows the technique explained elsewhere [11]. Briefly, to reconstruct Λ candidates, proton candidates are combined with charged tracks that are assumed to be pions. The $p\pi$ combination is required to be within 10 MeV of the known Λ mass and then is kinematically constrained to that value. Similarly, Ξ^- candidates are built from these Λ candidates with the addition of another appropriately charged track assumed to be a pion. The $\Lambda\pi$ vertex was required to be closer to the beamspot than the Λ decay point. The Σ^0 candidates were formed from the combination of Λ candidates and a cluster of greater than 50 MeV energy detected in the crystal calorimeter, not matched to the trajectory of a charged track, and consistent in shape with that expected from a photon. The Σ^+ and Ξ^0 reconstruction is complicated by the fact that we cannot use the beamspot for the point of origin of the photons. A kinematic fit is made to the hypothesis that the parent hyperon originated at the beamspot, and decayed after a positive path-length at a point taken to be the origin of the $\pi^0 \rightarrow \gamma\gamma$ decay. A requirement was placed on the χ^2 of the fit to

this topology, which includes the fit to the π^0 mass from the newly found decay vertex. In all cases, hyperon candidates within 3σ of their nominal masses are considered for further analysis, and their four-momenta are then constrained to the nominal hyperon mass. These kinematic constraints were sufficient to ensure that cross-feed background from real χ_{cJ} decays, for instance $\Lambda\bar{\Lambda}\pi^+\pi^-$ in the $\Xi^-\bar{\Xi}^-$ sample, was negligible.

For events with two distinct baryon candidates, we combine the candidates into a χ_c candidate. At this stage of the analysis, the invariant mass resolution of the χ_c is around 15 MeV/ c^2 . We then search for any unused photon in the event and add that to the χ_c candidate to form a $\psi(2S)$ candidate. This $\psi(2S)$ is then kinematically constrained to the four-momentum of the beam, the energy of which is calculated using the known $\psi(2S)$ mass. The momentum is non-zero due to the finite crossing angle (≈ 3 mrad per beam) in CESR. To make our final selection, we require the $\psi(2S)$ candidate to have a χ^2 of less than 25 for the four degrees of freedom for this fit; this requirement rejects most background combinations. This kinematic fit greatly improves the mass resolution of the χ_c candidate.

To study the efficiency and resolutions, we generated Monte Carlo samples for each χ_c into each final state using a GEANT-based detector simulation [12]. The simulated events have an angular distribution of $(1 + \alpha \cos^2 \theta)$, where θ is the radiated photon angle relative to the positron beam direction, and $\alpha = 1, -1/3$, and $1/13$ for the χ_{c0}, χ_{c1} , and χ_{c2} respectively, in accordance with expectations for an E1 transition. The mass resolution and efficiencies are shown in Table I. The resolutions are approximated by single Gaussian signal functions. The efficiencies shown include all the relevant branching fractions. [1]

TABLE I: Efficiencies (in %) obtained from analysis of Monte Carlo generated events, and yields found in the data sample.

Mode	χ_{c0}		χ_{c1}		χ_{c2}	
	Yield	Efficiency(%)	Yield	Efficiency (%)	Yield	Efficiency(%)
$p\bar{p}$	383 ± 22	62.4	141 ± 13	66.6	121 ± 12	65.5
$\Lambda\bar{\Lambda}$	131 ± 12	16.2	46.0 ± 7.2	17.1	71.0 ± 9.2	17.3
$\Sigma^0\bar{\Sigma}^0$	78 ± 10	4.1	3.8 ± 2.5	4.0	7.5 ± 3.4	4.0
$\Sigma^+\bar{\Sigma}^+$	39 ± 7	5.2	4.3 ± 2.3	5.0	4.0 ± 2.3	4.7
$\Xi^-\bar{\Xi}^-$	95 ± 11	7.7	16.4 ± 4.3	8.2	29 ± 5	8.4
$\Xi^0\bar{\Xi}^0$	23.3 ± 4.9	2.9	1.7 ± 1.4	2.9	2.9 ± 1.7	2.9

The final invariant mass distributions are shown in Fig. 1. These plots are each fit with three signal shapes comprising Breit-Wigner functions convolved with Gaussian resolutions, together with a constant background term. The masses and widths of the Breit-Wigner functions were fixed according to the current averages [1], and the widths of the Gaussian resolution functions were fixed at the values found from Monte Carlo simulation (ranging from 3.6-5.1 MeV/ c^2 depending on the spin of the χ_c and the decay mode). The yields from these fits are tabulated in Table I.

To convert the yields to branching fractions, we divide by the product of the number of $\psi(2S)$ events in the data sample, the detector efficiency, and the branching fractions for $\psi(2S)$ into χ_{cJ} . For the last factor we use the CLEO measurements of $\mathcal{B}(\psi(2S) \rightarrow \gamma\chi_{c0}) = 9.22 \pm 0.11 \pm 0.46\%$, $\mathcal{B}(\psi(2S) \rightarrow \gamma\chi_{c1}) = 9.07 \pm 0.11 \pm 0.54\%$, and $\mathcal{B}(\psi(2S) \rightarrow \gamma\chi_{c2}) = 9.33 \pm 0.14 \pm 0.61\%$ [8]. The results are tabulated in Table II.

We consider systematic uncertainties from many different sources. All modes have a 2%

uncertainty from the total number of $\psi(2S)$ decays [8]. The requirement on the χ^2 of the constraint to the beam four-momentum has been checked by changing the cut and noting the change in the yield in these, and other similar decay modes. Based on this study we place a systematic uncertainty of 2.5% on the efficiency of this requirement. The uncertainties due to track reconstruction are 0.3% per charged track. The limited Monte Carlo statistics introduces an uncertainty that is always a small fraction of the statistical uncertainty in the data. Using comparison of data and Monte Carlo simulation of hyperon and anti-hyperon yields from the $\psi(2S)$, we checked our modeling of the hyperon selection efficiency. The assigned systematic uncertainty arising from this study was up to 3% per hyperon. The systematic uncertainty due to the photon detection and shower-shape criteria is set at 2% per photon. In the case of the χ_{c1} decaying into two spin one-half particles, the two daughters can have their spins either parallel or antiparallel, and in the χ_{c2} case there are even more possibilities of combinations of intrinsic spins and relative angular momentum. These helicity correlations are not well known in the case of decays into baryons, and this introduces a small uncertainty in the modeling of the efficiencies. We investigated the effects of helicity amplitudes on our efficiency by generating Monte Carlo with a variety of different helicities and found small variations. From this study, we assign a 1% uncertainty in the efficiency of the χ_{c1} and 2.5% of the χ_{c2} . When calculating the final branching fractions, we add the above systematic uncertainties in quadrature. The uncertainty due to the $\psi(2S) \rightarrow \gamma\chi_c$ branching fractions is kept separate and quoted as a second systematic uncertainty.

For evaluating the limits in the cases where there is no significant signal, we take the probability density function and convolve this with Gaussian systematic uncertainties. We then find the branching fraction that includes 90% of the total area.

TABLE II: Branching fraction results (in units of 10^{-5}) for each decay mode. The uncertainties are statistical, systematic due to this measurement, and systematic due to the $\psi(2S) \rightarrow \chi_{cJ}\gamma$ rate, respectively. The limits on the branching fractions include all systematic uncertainties.

Mode		χ_{c0}	χ_{c1}	χ_{c2}
$p\bar{p}$	This Work	$25.7 \pm 1.5 \pm 1.5 \pm 1.3$	$9.0 \pm 0.8 \pm 0.4 \pm 0.5$	$7.7 \pm 0.8 \pm 0.4 \pm 0.5$
	PDG	22.5 ± 2.7	7.2 ± 1.3	6.8 ± 0.7
$\Lambda\bar{\Lambda}$	This Work	$33.8 \pm 3.6 \pm 2.2 \pm 1.7$	$11.6 \pm 1.8 \pm 0.7 \pm 0.7$	$17.0 \pm 2.2 \pm 1.1 \pm 1.1$
	PDG	47.0 ± 16.0	26.0 ± 12.0	34.0 ± 17.0
$\Sigma^0\bar{\Sigma}^0$	This Work	$44.1 \pm 5.6 \pm 4.2 \pm 2.2$	< 4.4	< 7.5
	PDG			
$\Sigma^+\bar{\Sigma}^+$	This Work	$32.5 \pm 5.7 \pm 4.0 \pm 1.7$	< 6.5	< 6.7
	PDG			
$\Xi^-\bar{\Xi}^-$	This Work	$51.4 \pm 6.0 \pm 3.9 \pm 2.6$	$8.6 \pm 2.2 \pm 0.6 \pm 0.5$	$14.5 \pm 3.0 \pm 1.2 \pm 0.9$
	PDG	$< 103^a$	< 34	< 37
$\Xi^0\bar{\Xi}^0$	This Work	$33.4 \pm 7.0 \pm 4.5 \pm 1.7$	< 6.0	< 10.6
	PDG			

^aThe BES central value [13] for this measurement is $(53 \pm 27 \pm 9) \times 10^{-5}$, in good agreement with this work.

In summary, we measure branching fractions for χ_{c0} decays into $p\bar{p}$, $\Lambda\bar{\Lambda}$, $\Xi^-\bar{\Xi}^-$, $\Xi^0\bar{\Xi}^0$, $\Sigma^0\bar{\Sigma}^0$ and $\Sigma^+\bar{\Sigma}^+$. For χ_{c1} and χ_{c2} we find significant signals and measure branching fractions into the first three of the above decay modes. Upper limits on branching fractions

are obtained for the remainder of the modes. In the case of $\chi_{cJ} \rightarrow p\bar{p}$ and $\chi_{cJ} \rightarrow \Lambda\bar{\Lambda}$, these measurements are the most precise to date; in the other modes they represent first measurements. Our values of the branching fractions for $\Lambda\bar{\Lambda}$ are well below those reported by BES, but confirm the trend that the branching fractions into $\Lambda\bar{\Lambda}$ are higher than those for $p\bar{p}$. The fact that the χ_{c0} branching fractions into $\Sigma\bar{\Sigma}$ and $\Xi\bar{\Xi}$ are all greater than that of $\chi_{c0} \rightarrow p\bar{p}$, a trend not mirrored in the χ_{c1} and χ_{c2} decays, is not in agreement with naive expectations for the decay of an SU(3) singlet.

We gratefully acknowledge the effort of the CESR staff in providing us with excellent luminosity and running conditions. D. Cronin-Hennessy and A. Ryd thank the A.P. Sloan Foundation. This work was supported by the National Science Foundation, the U.S. Department of Energy, the Natural Sciences and Engineering Research Council of Canada, and the U.K. Science and Technology Facilities Council.

-
- [1] W.-M. Yao *et al.* (Particle Data Group), *J. Phys. G* **33**, 1 (2006).
 - [2] S. J. Brodsky and G. P. Lepage, *Phys. Rev. D* **24**, 2848 (1981).
 - [3] G. T. Bodwin, E. Braaten, and G. P. Lepage, *Phys. Rev. D* **51** 1125 (1995).
 - [4] S.M.H. Wong, *Eur. Phys. J.* **C14**, 643 (2000).
 - [5] J. Bai *et al.* (BES Collaboration), *Phys. Rev. D* **67**, 112001 (2003).
 - [6] R. G. Ping, B. S. Zou, and H. C. Chiang, *Eur. Phys. J.* **A23**, 129 (2004).
 - [7] R.A. Briere *et al.* (CESR-c and CLEO-c Taskforces, CLEO-c Collaboration), Cornell University, LEPP Report No. CLNS 01/1742 (2001) (unpublished), G. Viehhauser *et al.*, *Nucl. Instrum. Meth. A* **462**, 146 (2001).
 - [8] H.Mendez *et al.* (CLEO Collaboration), *Phys. Rev. D* (submitted), arXiv:0804.4432 [hep-ex].
 - [9] Y. Kubota *et al.* (CLEO Collaboration), *Nucl. Instrum. Methods Phys. Res., Sect. A* **320**, 66 (1992).
 - [10] M. Artuso *et al.*, *Nucl. Instrum. Meth. Phys. Res., Sect. A* **554**, 147 (2005).
 - [11] T. K. Pedlar *et al.* (CLEO Collaboration), *Phys. Rev. D* **72**, 051108 (2005).
 - [12] R. Brun *et al.* (Geant) 3.21, CERN Program Library Long Writeup W5013 (1993), unpublished.
 - [13] J. Z. Bai *et al.* (BES Collaboration), *Phys. Rev. D* **73**, 052006 (2006).

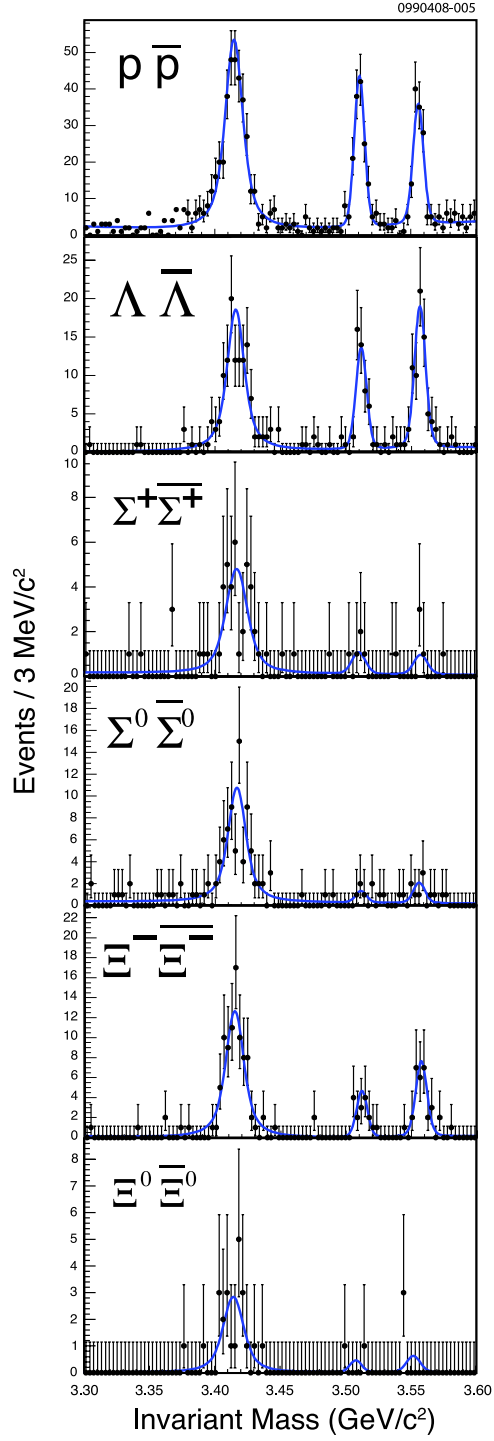


FIG. 1: Invariant mass distributions for $p\bar{p}$, $\Lambda\bar{\Lambda}$, $\Sigma^0\bar{\Sigma}^0$, $\Sigma^+\bar{\Sigma}^+$, $\Xi^-\bar{\Xi}^-$, $\Xi^0\bar{\Xi}^0$. The fits are described in the text.